https://doi.org/10.1016/j.aca.2017.05.026

Chiral Differentiation of Amino Acids through Binuclear Copper Bound Tetramers by Ion Mobility Mass Spectrometry

XiangyingYu[a,b], Zhong-Ping Yao[b,c,d*]

[a]College of Pharmacy, Jinan University, Guangzhou 510632, Guangdong, China

[b]State Key Laboratory of Chinese Medicine and Molecular Pharmacology (Incubation) and Shenzhen Key Laboratory of Food Biological Safety Control, Shenzhen research institute of Hong Kong Polytechnic University, Shenzhen 518057, China

[c]Key Laboratory of Natural Resources of Changbai Mountain and Functional Molecules (Yanbian University), Ministry of Education, Yanji 133002, Jilin, China

[d]State Key Laboratory of Chirosciences, Food Safety and Technology Research Centre and Department of Applied Biology and Chemical Technology, The Hong Kong Polytechnic University, Hung Hom, Kowloon, Hong Kong Special Administrative Region, China

[*]Corresponding author.
Tel: +852 34008792, fax: +852 2364 9932, email address: zhongping.yao@polyu.edu.hk

Abstract

In this study, travelling wave ion mobility mass spectrometry has been used to investigate chiral differentiation of common chiral amino acids, through separation of binuclear copper bound tetrameric ions formed with chiral selector tryptophan, proline, tyrosine, phenylalanine or histidine. Significant chiral recognition was observed for amino acids with aromatic rings or long and active side chains, with peak-to-peak resolutions up to 1.826. Tryptophan and histidine offered better enantioselectivity, compared to other chiral selectors. The results suggested that the mechanism for chiral recognition in ion mobility mass spectrometry might be significantly different from that in tandem mass spectrometry. Linear calibration curves were also established to allow determination of enantiomeric excess of the analytes by the approach. This study showed that higher assembly of chiral analyte and chiral selector might enable better chiral discrimination and ion mobility mass spectrometry could be a powerful technique for provide qualitative, quantitative and structural information of chiral analysis.

Keywords: Ion mobility mass spectrometry; chiral recognition; determination of enantiomeric excess; binuclear copper bound tetrameric ions; amino acids.

1. Introduction

Chiral recognition is of great importance in chemical, biological, and pharmaceutical sciences. Since the first observation of chirality effect in mass spectrometry (MS) in 1977 [1], MS has played a growing role in chiral recognition due to its significant advantages in speed, sensitivity and specificity. Traditionally, a chiral selector is used to form diastereomers with the analyte enantiomers, and chiral recognition by mass spectrometry is based on comparison of generation of diastereomers in single-stage MS or dissociation of diastereomers in tandem MS [2-11].

Recently, ion mobility mass spectrometry (IM-MS) has been developed as a new approach for chiral differentiation, which could be achieved by the mobility difference, i.e., drift time difference, of analyte enantiomers in the presence of a chiral selector in drift cell [12] or diastereomers incorporating the chiral selector and enantiomer analytes [13-15]. For a pair of diastereomeric ions, which are of the same mass-to-charge ratio (m/z), their ion mobility difference is caused by the difference of their collision cross sections (CCSs), which are dependent on their sizes and shapes [16, 17]. Compared to other MS-based approaches for chiral differentiation, IM-MS could allow chiral recognition and enantiomeric excess determination to be completed in a single measurement without the need of isotopic labelling to the enantiomers, and could provide structural information

of enantiomeric or diastereomeric ions through measurements of their CCSs [12-15]. IM-MS is thus a very promising technique for chiral analysis. In 2006, Dwivedi et al. [12] used drift tube ion mobility mass spectrometry (DTIM-MS) with (S)-(+)-2-butanol as the drift gas modifier for chiral separation of compounds, including atenolol, serine, methionine, threonine, methyl α-glucopyranoside, glucose, penicillamine, valinol, phenylalanine, and tryptophan. After that, there have been only a few publications in chiral study by IM-MS, including chiral differentiation of six amino acids and terbutaline by field asymmetric waveform ion mobility mass spectrometry (FAIM-MS) [13, 14], and chiral differentiation of tyrosine and tryptophan by travelling wave ion mobility mass spectrometry (TWIM-MS) [15]. The diastereomer ions involved in these studies [13-15] were typically trimers of analytes and chiral selectors bound with one metal ion. It is worth noting that, despite the larger IM resolution of FAIM-MS than TWIM-MS in the present commercial instruments, TWIM-MS allows calculation of CCSs while CCSs could not be determined by FAIM-MS [16].

Considering the significant advantages and very limited applications of IM-MS in chiral differentiation, in this work, IM-MS-based chiral analysis was further explored by using TWIM-MS to investigate diastereomers with higher assembly of analytes, chiral selectors and metal ions, which could enable larger difference in CCSs and thus more significant chiral discrimination. Cu^{2+} was chosen as the metal ion in the study due to its coordination properties and favorable performance in the previously reported

chiral recognition [18-20]. Moreover, the relationship and linear calibration curve for determination of enantiomeric excess (ee) using the IM-MS approach were clarified and established in this study. The developed approach in this study was based on TWIM-MS that could allow CCS determination and thus provide structural information of the study ions, and is applicable with other IM-MS techniques, such as DTIM-MS and FAIM-MS that may be able to provide larger IM resolutions and better separation performance.

2. Experimental

2.1. Chemicals

All optically pure chiral amino acids and $CuCl_2$ were purchased from Aladdin (Shanghai, China), and methanol was of HPLC grade and purchased from BCR International Trading Ltd. Co (California,USA). All chemicals were used directly without further purification.

2.2. Sample preparation

Chiral amino acids and $CuCl_2$ were dissolved separately in water to achieve a concentration of 500 μM each. The sample solution used for IM-MS analysis was prepared by mixing the stock solution and then diluting with 50/50 water/methanol, to obtain a final solution containing 20 μM analyte amino acid (X), 20 μM chiral selector (Y) and 20 μM transition metal ion ($CuCl_2$) These concentrations were employed after the optimization for generation of binuclear copper bound complex ions with higher

abundances.

2.2. Electrospray ionization traveling wave ion mobility mass spectrometry (ESI-TWIM-MS) analysis

The analytical procedure for the approach is shown in Fig. S1. The IM-MS experiments were carried out by directly infusing sample solutions at a flow rate of 10 μL/min into Q-IM-TOF mass spectrometer (Synapt G2 HDMS, Waters) under the positive electrospray ionization. ESI conditions were as follows: capillary voltage 3 kV, sampling cone 30-50 V, extraction cone 5 V, source temperature 100 °C, desolvation temperature 350 °C, cone gas 50 L/h, and desolvation gas 500 L/h. IM conditions were as follows: drift gas N_2, traveling wave height 40 V, and velocity 600 m/s. For MS/MS analysis, the transfer collision energy was set to a value for which the intensity ratio of product ion to precursor ion was close to unity for one enantiomer of the analyte.

The CCS values of the investigated complexes were calculated by using polyalanines with a concentration of 10 μg/mL to plot a calibration curve as described by the literature [17], and the CCS values of polyalanines were obtained from the online CCS database [21].

3. Results and discussion

3.1. Complex ions detected

Electrospray ionization has been shown to be able to effectively generate copper bound complex ions, including ions of copper bound dimers, copper bound trimers, etc., from aqueous methanol solutions containing Cu^{2+} and ligands [22-25]. Under the experimental conditions in this study, mainly sodium-based cluster ions were observed in the ESI mass spectra of Cu^{2+} and amino acid mixtures. Fig. 1 shows a typical mass spectrum of the sample solutions. Except for the copper bound dimer and trimer ions, the binuclear copper bound complex ions $[(Cu^{2+})_2XY_3\text{-}4H+Na]^+$, $[(Cu^{2+})_2X_2Y_2\text{-}4H+Na]^+$ and $[(Cu^{2+})_2X_3Y\text{-}4H+Na]^+$ were also observed and identified through accurate monoisotopic masses and isotopic patterns (see Fig. S2). Generation of binuclear copper bound complex ions was found to be dependent on the amino acid studied. No binuclear copper bound complex ion was observed for Cys (see Fig. S3b), due to the easy oxidation of Cys to cystine under such conditions [26]. Complex ions $[(Cu^{2+})_2XY_2\text{-}4H+Na]^+$ could also be observed in the sample solutions containing analyte glutamic acid (Glu) and aspartic acid (Asp) (see Fig. S3c&d), presumably due to the presence of the additional carboxyl group in Glu and Asp; while complex ions $[(Cu^{2+})_2XY_3\text{-}3H]^+$ were observed with high abundances in the sample solutions containing analyte arginine (Arg) (see Fig. S3a), probably due to the significantly high proton affinity of Arg [27, 28].

For the sodium-based copper bound dimer and trimer ions, our preliminary results with TWIM-MS analysis showed no significant chiral discrimination for the amino acids investigated (see Tables S1 and S2 in the Supporting Information). A recent report also indicated that the diastereomeric copper bound trimeric ions were of limited application in TWIM-MS-based chiral recognition of amino acids [15]. Diastereomeric binuclear copper bound tetrameric ions, which are of higher assembly of analytes, chiral selectors and metal ions and thus might enable larger difference in CCSs and consequently more significant chiral discrimination, however, has not been reported for chiral recognition yet. IM-MS analysis of binuclear copper bound tetrameric ions for chiral recognition of common amino acids was therefore focused in this study. For complex ions containing more than one analyte molecule, e.g., $[(Cu^{2+})_2X_2Y_2\text{-}4H+Na]^+$ and $[(Cu^{2+})_2X_3Y\text{-}4H+Na]^+$, when both of the two enantiomers are present in the sample solutions, heterochiral analytes ($^{L}X+^{D}X$) and homochiral analytes ($^{L}X+^{L}X$ or $^{D}X+^{D}X$) could co-exist in the complex ions, leading to the complexity in chiral analysis. To avoid this, only complex ions containing one analyte molecule, i.e., $[(Cu^{2+})_2XY_3\text{-}4H+H/Na]^+$, were chosen for the study. L-tryptophan (Trp), L-proline (Pro), L-tyrosine (Tyr), L-phenylalanine (Phe) and L-histidine (His) were chosen as the chiral selectors since significant enantioselectivity was observed for these five amino acids in the previous studies [29-31].

3.2. Chiral recognition of amino acids through separation of binuclear copper bound tetrameric ions in TWIM-MS

Chiral discrimination was achieved when the binuclear copper bound tetrameric ions of the two enantiomers were separated in the IM-MS spectra. To describe the chiral discrimination in the IM-MS spectra, the differences in the drift time and CCSs of diastereomeric ions, as well as the peak-to-peak resolution ($R_{p\text{-}p}$) were measured and shown in Table 1. $R_{p\text{-}p}$ was calculated by equation (1),

$$R_{p\text{-}p} = \frac{|t_D - t_L|}{1/2(W_D + W_L)} \quad (1)$$

where t_D and t_L as well as W_D and W_L refer to the drift time as well as the peak width of diastereomeric ions of the D and L-analyte, respectively. Such a definition is similar to the definition of column resolution in chromatography, and the larger $R_{p\text{-}p}$ value indicates the higher chiral discrimination. Drift time difference and peak-to-peak resolution are two important factors for describing peak separation in the ion mobility spectra, while the latter takes into account of the peak width that can be increased with ion diffusion and other factors [15, 32]. Normally, a larger CCS difference of the diastereomeric ions corresponds to a larger $R_{p\text{-}p}$ value. In this approach, the concentration of $CuCl_2$ is related to the intensities of the diastereomeric ions but has no significant influence on CCS difference, i.e., drift time difference, and thus the discrimination efficiency (see Table S5). This is different from the chromatography-based chiral separation, which is influenced by the concentration of the metal ions [33].

The significantly separated binuclear copper bound diastereomeric ions were summarized in Table 1, with the IM-MS spectra shown in Fig. 2 and Fig. 3 (see Table S3 for the results of the unseparated complex ions). Significant chiral discriminations were observed for Trp, glutamine (Gln), Tyr and threonine (Thr) with His as the chiral selector, for His with Phe or Tyr as the chiral selector, for Gln, Tyr, Glu, methionine (Met) and Phe with Trp as the chiral selector, and for Glu and Arg with Tyr as the chiral selector. Compared to the previous use of trimeric ions bound with one copper ion in TWIM-MS for chiral differentiation of common amino acids, which only allowed successful chiral differentiation of two amino acids (Trp, Tyr) with the largest resolution of 0.60 [15], the use of binuclear copper bound tetrameric ions in this study could allow successful chiral differentiation of much more amino acids with resolutions up to 1.826 (for Trp with His as the chiral selector), suggesting that the binuclear copper bound tetramers were better diastereomers for chiral differentiation of amino acids with the technique. Among various examined amino acid analytes, obvious chiral differentiation could only be achieved for those possessing aromatic rings or long side chains with active groups such as OH, NH_2, COOH and S, suggesting the important roles of aromatic rings as well as long and active side chains in the chiral discrimination.

Among the five chiral selectors, Pro showed no significant chiral discriminations, and Trp and His showed the best chiral discrimination ability toward a wider variety of amino acids, presumably due to the additional binding site provided by the imidazole

ring of His or indole ring of Trp for the interactions between amino acids and Cu(II) [34] as well as the stronger affinity of His and Trp with Na^+ [28]. However, when both His and Trp were together used as the chiral selectors for chiral recognition of the amino acids, chiral discrimination, through the separation of diastereomeric binuclear copper bound teterameric ions ($[(Cu^{2+})_2X(His)(Trp)_2\text{-}4H+Na]^+$ or $[(Cu^{2+})_2X(His)_2(Trp)\text{-}4H+Na]^+$) in the IM-MS spectra, was observed only for Gln and Tyr and with the resolutions lower than those obtained when using His or Trp alone as the chiral selector (see Table S4), suggesting that combination of these two chiral selectors might be not better than the single one for the chiral recognition and that the chiral recognition mechanism needs further study. In addition, it could also be found from Fig. 2 and Fig. 3 that for the diastereomeric binuclear copper bound teterameric ions $[(Cu^{2+})_2XY_3\text{-}4H+Na]^+$, when His or Trp was used as the chiral selector, the heterochiral (i.e., analyte and chiral selector of the opposite configurations) complex ions had larger sizes than their corresponding homochiral (i.e., analyte and chiral selector of the same configuration) complex ions, and when Tyr or Phe was used as the chiral selector, homochiral complex ions had larger sizes than their corresponding heterochiral complex ions (including for $[(Cu^{2+})_2{}^{L/D}Glu(^{L}Tyr)_2\text{-}4H+Na]^+$).

It was also interesting to note that Na^+ adduct ions of diastereomers did not always lead to better chiral differentiation than the protonated ions. For Arg with Tyr as the chiral selector, $[(Cu^{2+})_2(Arg)(Tyr)_3\text{-}3H]^+$ rather than the corresponding Na^+ adduct ion (see Table S3) was selected for the chiral differentiation due to the higher discrimination

ability of the former. This might be related to the significantly higher proton affinity of Arg than other amino acids, and the binding preference of Arg zwitterion structure with sodium ion [27, 28, 35], which could reduce the structural difference and thus the CCS difference between the homochiral and heterochiral complexes.

3.3. Comparison with chiral recognition by tandem mass spectrometry

MS/MS-based approach, i.e., collision-induced dissociation (CID) of diastereomeric ions, has been more commonly used for chiral recognition. In this study, MS/MS-based chiral recognition of the binuclear copper bound teterameric ions with Trp as the chiral selector was investigated, to compare with the results obtained with IM-MS. Some MS/MS spectra are shown in Fig. S4. Comparison of the intensity ratio of $[(Cu^{2+})_2(X)(Trp)_2\text{-}4H+Na]^+$ to $[(Cu^{2+})_2(X)(Trp)_3\text{-}4H+Na]^+$ of the two enantiomers (with a value larger than unity) was used to indicate the enantioselectivity, unless the product ions could not be effectively detected. In this case, an enantioselectivity value closer to unity indicates a smaller chiral discrimination. The MS/MS results for chiral recognition of the common amino acids are summarized in Table 2. Different from the results obtained by using the trimeric ions [22, 30, 31, 36], for $[(Cu^{2+})_2(^{L/D}X)(^{L}Trp)_3\text{-}4H+Na]^+$ ions, r_D larger than r_L was obtained for all amino acids except for Leu, indicating that dissociation was more favorable for the heterochiral complexes and that the homochiral complexes were more stable than the heterochiral complexes. As shown in Table 2, significant chiral

discriminations were observed for Pro, Met, Ser and other amino acids except for those having alkyl side chains, i.e., Ala, Ile, Leu and Val. This results was similar with the results obtained by using the kinetic method to study the dissocition of trimeric ions [22, 30, 31, 36], suggesting the important role of rigid structure in the MS/MS-based stereospecificity and that the functional group on the side chains of amino acids might interact with copper ion, which contributed to the chiral recognition [36].

Compared with the IM-MS approach for the same system that allowed significant chiral discrimination of only five amino acids Gln, Tyr, Glu, Met and Phe, the MS/MS approach enabled significant chiral discrimination for most of the common amino acids. This is believed to be related with the low ion mobility resolution of the current IM-MS equipment, which cannot distinguish two very close peaks in the IM-MS spectra. For the five amino acids that could be differentiated with the IM-MS approach, their enantioselectivity values were generally not the highest with the MS/MS approach. Pro and Ser were the two amino acids with the most significant enantioselectivity with the MS/MS approach. Pro has a very rigid structure and was found to be favourable for the MS/MS-based chiral recognition [6, 7, 36]. However, no obvious chiral discriminations were observed with the IM-MS approach when Pro was used as the chiral selector or analyte. The discrepancy of chiral recognition between the MS/MS approach and IM-MS approach suggested that the two approaches might

be based on very different mechanisms for chiral differentiation. The MS/MS-based chiral recognition might be more based on the energy difference of the diastereomeric complexes, which is more sensitive to the structural rigidness and active group in the diastereomeric complexes, while the IM-MS-based chiral recognition might be more dependent on the size and shape difference of the diastereomeric complexes, which is more sensitive to more flexible or extended structures such as those with aromatic rings, long and active side chains and higher assembly.

3.4. Determination of enantiomeric excess (ee)

The utility of IM-MS analysis for ee determination of amino acids was also investigated in this study. Since *r*, the peak area ratio of the two separated diastereomeric binuclear metal bound tetrameric ions in the ion mobility mass spectrum, is proportional to the concentration ratio of the two enantiomer analytes in the sample solution, equation (2) could be obtained,

$$r = \frac{[\text{Diastereo}]_{\text{L}}}{[\text{Diastereo}]_{\text{D}}} = k\frac{C_L}{C_D} \tag{2}$$

where $[\text{Diastereo}]_{\text{L}}$ and $[\text{Diastereo}]_{\text{D}}$ refer to the peak area of the diastereomeric complex ions of the L and D-analyte, respectively, C_L and C_D refer to the original concentration of L and D-analyte, respectively, and *k* is the proportional constant, which is associated with the generation and ionization efficiency of the diastereomeric complex ions, etc.

According to the definition of enantiomeric excess (ee), equation (3) can be obtained:

$$\mathrm{ee} = \frac{C_L - C_D}{C_L + C_D} \times 100 \tag{3}$$

Equation (3) can be transformed into:

$$\mathrm{ee} = \frac{C_L / C_D - 1}{C_L / C_D + 1} \times 100 \tag{4}$$

Solving equation (4),one can get:

$$C_L / C_D = \frac{100 + \mathrm{ee}}{100 - ee} \tag{5}$$

Equation (2) can then be transformed to:

$$r = k \cdot \frac{100 + \mathrm{ee}}{100 - \mathrm{ee}} = k \cdot \frac{-(100 - \mathrm{ee}) + 200}{100 - \mathrm{ee}} = -k + \frac{200k}{100 - \mathrm{ee}} \tag{7}$$

Therefore, a linear calibration curve for ee determination could be obtained by ploting *r* versus 1/(100-ee).

By setting r_0 as the *r* value of the racemic sample, i.e., ee = 0, then r_0 can be obtained from equation (7):

$$r_0 = k \tag{8}$$

Substituting equation (7) with equation (8), equation (9) can be obtained:

$$r - r_0 = -2k + \frac{200k}{100 - \mathrm{ee}} = \frac{2k \cdot \mathrm{ee}}{100 - \mathrm{ee}} \tag{9}$$

Taking the reciprocal, equation (9) can be transformed into equation (10):

$$\frac{1}{r - r_0} = \frac{100 - \mathrm{ee}}{2k \cdot \mathrm{ee}} = \frac{50}{k} \cdot \frac{1}{\mathrm{ee}} - \frac{1}{2k} \tag{10}$$

A linear calibration curve for the ee determination could thus be also obtained by

ploting $1/(r\text{-}r_0)$ versus 1/ee, which has been well established in the MS/MS-based chiral analysis, where *r* is the intensity ratio between product ion and precursor ion [37].

In this study, samples containing different ee of amino acid analyte were mixed with $CuCl_2$ and the chiral selector for IM-MS analysis. Three amino acids Trp, Arg and Glu with diastereomeric ions $[(Cu^{2+})_2{}^{L/D}Trp(^{L}His)_3\text{-}4H+Na]^+$, $[(Cu^{2+})_2{}^{L/D}Arg(^{L}Tyr)_3\text{-}3H]^+$ and $[(Cu^{2+})_2{}^{L/D}Glu(^{L}Tyr)_2\text{-}4H+Na]^+$, respectively, were investigated for demonstration in this study. Linear calibration curves with R^2 values better than 0.99 were obtained for all these investigated analytes by plotting *r* against 1/(100-ee) (see Figs. 4b, 4d and 4f), or $1/(r\text{-}r_0)$ against 1/ee (see Fig. S5), demonstrating the feasibility of the method for ee determination. It can be seen from the plots that smaller measurement errors, as indicated by the error bars in the plots, tended to be obtained with the larger $R_{p\text{-}p}$ values.

To detect the precision and repeatability of this IM-MS method, five Trp samples with different ee were mixed with L-His and $CuCl_2$ for IM-MS analysis with six repeated measurements for each sample. As shown in Table 3, except for the sample with 0% ee, which showed a relatively large error of 2.07% ee, the absolute errors were less than 1% ee for other samples, and the RSD values for all the measurement were less than 7%.

4. Conclusions

In summary, we demonstrated chiral recognition and optical purity determination of amino acids by IM-MS through binuclear copper bound tetrameric ions. The results

indicated that binuclear copper bound tetrameric ions showed higher CCS differences between the diastereomers than the commonly used trimers bound with one copper ion and were promising species for chiral differentiation, suggesting the potential of diastereomers with higher assembly for more significant chiral recognition. It was found that the binuclear copper bound tetrameric diastereomers formed by amino acids with aromatic rings or long and active side chains tended to have larger CCS differences and thus better enantioselectivity. Our results also suggested that the mechanism of chiral recognition by IM-MS might be very different from that by MS/MS, providing new strategy for designing chiral recognition systems for the two approaches. Additionally, a quantitation method for determining the enantiomeric excess (ee) of analyte was developed based on the linear calibration curve between r and 1/(100-ee) or the linear calibration curve between $1/(r-r_0)$ and 1/ee. The results indicate that IM-MS is a very promising approach for chiral analysis, particularly with the improvement of ion mobility resolution of the equipment in the future, and the present approach can be extended for chiral analysis of other sample systems such as drugs and sugars. Theoretical calculations of the binuclear metal bound complexes would be performed for better understanding the interactions in binuclear metal bound complexes and the mechanism for the chiral discrimination.

Acknowledgements

This research was supported by Collaborative Research Fund of Hong Kong Research Grants Council (Grant No. C5031-14E), State Key Laboratory of Chirosciences, and

The University Research Facility in Chemical and Environmental Analysis (UCEA) of The Hong Kong Polytechnic University.

References

[1] H.M. Fales, G.J. Wright, Detection of chirality with chemical ionization mass-spectrometer - meso ions in gas phase, J. Am. Chem. Soc., 99 (1977) 2339-2340.

[2] K.A. Schug, N.M. Maier, W. Lindner, Chiral recognition mass spectrometry: remarkable effects observed from the relative ion abundances of ternary diastereomeric complexes using electrospray ionization, Chem. Commun., (2006) 414-416.

[3] C.L. Zu, J.A. Woolfolk, M.E. Koscho, Enantiomer assays of amino acid derivatives using tertiary amine appended trans-4-hydroxyproline derivatives as chiral selectors in the gas phase, Anal. Chim. Acta, 661 (2010) 60-66.

[4] H. Fleischer, K. Thurow, Fast mass spectrometry-based enantiomeric excess determination of proteinogenic amino acids, Amino Acids, 44 (2013) 1039-1051.

[5] C. Fraschetti, M.C. Letzel, M. Paletta, J. Mattay, M. Speranza, A. Filippi, M. Aschi, A.B. Rozhenko, Cyclochiral resorcin[4]arenes as effective enantioselectors in the gas phase, J. Mass Spectrom., 47 (2012) 72-78.

[6] Z.P. Yao, T.S.M. Wan, K.P. Kwong, C.T. Che, Chiral recognition of amino acids by electrospray ionisation mass spectrometry/mass spectrometry, Chem. Commun., (1999) 2119-2120.

[7] Z.P. Yao, T.S.M. Wan, K.P. Kwong, C.T. Che, Chiral analysis by electrospray ionization mass spectrometry/mass spectrometry. 1. Chiral recognition of 19 common amino acids, Anal. Chem., 72 (2000) 5383-5393.

[8] L. Wang, Y.F. Chai, Z.Q. Ni, L. Wang, R.L. Hu, Y.J. Pan, C.R. Sun, Qualitative and quantitative analysis of enantiomers by mass spectrometry: Application of a simple chiral chloride probe via rapid in-situ reaction, Anal. Chim. Acta, 809 (2014) 104-108.

[9] A. Fujihara, N. Maeda, S. Hayakawa, Quantitative chiral analysis of tryptophan using enantiomer-selective photolysis of cold non-covalent complexes in the gas phase, J. Mass Spectrom., 50 (2015) 451-453.

[10] R.M. Bain, X. Yan, S.A. Raab, S.T. Ayrton, T.G. Flick, R.G. Cooks, On-line

chiral analysis using the kinetic method, Analyst, 141 (2016) 2441-2446.

[11] X. Yu, Z. Yao, Chiral recognition and determination of enantiomeric excess by mass spectrometry: A review, Anal. Chim. Acta, 968 (2017) 1-20.

[12] P. Dwivedi, C. Wu, L.M. Matz, B.H. Clowers, W.F. Siems, H.H. Hill, Gas-phase chiral separations by ion mobility spectrometry, Anal. Chem., 78 (2006) 8200-8206.

[13] A. Mie, M. Jornten-Karlsson, B.O. Axelsson, A. Ray, C.T. Reimann, Enantiomer separation of amino acids by complexation with chiral reference compounds and high-field asymmetric waveform ion mobility spectrometry: preliminary results and possible limitations, Anal. Chem., 79 (2007) 2850-2858.

[14] A. Mie, A. Ray, B.O. Axelsson, M. Jornten-Karlsson, C.T. Reimann, Terbutaline enantiomer separation and quantification by complexation and field asymmetric ion mobility spectrometry-tandem mass spectrometry, Anal. Chem., 80 (2008) 4133-4140.

[15] V. Domalain, M. Hubert-Roux, V. Tognetti, L. Joubert, C.M. Lange, J. Rouden, C. Afonso, Enantiomeric differentiation of aromatic amino acids using traveling wave ion mobility-mass spectrometry, Chem. Sci., 5 (2014) 3234-3239.

[16] F. Lanucara, S.W. Holman, C.J. Gray, C.E. Eyers, The power of ion mobility-mass spectrometry for structural characterization and the study of conformational dynamics, Nat. Chem., 6 (2014) 281-294.

[17] D.P. Smith, T.W. Knapman, I. Campuzano, R.W. Malham, J.T. Berryman, S.E. Radford, A.E. Ashcroft, Deciphering drift time measurements from travelling wave ion mobility spectrometry-mass spectrometry studies, Eur. J. Mass Spectrom., 15 (2009) 113-130.

[18] L.M. Wu, W.A. Tao, R.G. Cooks, Ligand and metal-ion effects in metal-ion clusters used for chiral analysis of alpha-hydroxy acids by the kinetic method, Anal. Bioanal. Chem., 373 (2002) 618-627.

[19] S. Kumari, S. Prabhakar, M. Vairamani, C.L. Devi, G.K. Chaitanya, K. Bhanuprakash, Chiral discrimination of D- and L-amino acids using iodinated tyrosines as chiral references: effect of iodine substituent, J. Am. Soc. Mass Spectrom., 18 (2007) 1516-1524.

[20] M.K. Lee, A.P. Kumar, D. Jin, Y.I. Lee, Determination of enantiomeric compositions of DOPA by tandem mass spectrometry using the kinetic method with fixed ligands, Rapid Commun. Mass Spectrom., 22 (2008) 909-915.

[21] Cross section database, http://www.indiana.edu/~clemmer/Research/Cross%20Section%20Database/c

s_database.php, (accessed October, 2016).

[22] R. Karthikraj, R.K. Chitumalla, K. Bhanuprakash, S. Prabhakar, M. Vairamani, Enantiomeric differentiation of beta-amino alcohols under electrospray ionization mass spectrometric conditions, J. Mass Spectrom., 49 (2014) 108-116.

[23] R. Karthikraj, S. Prabhakar, M. Vairamani, Differentiation of enantiomeric drugs by iodo-substituted L-amino acid references under electrospray ionization mass spectrometric conditions, Rapid Commun. Mass Spectrom., 26 (2012) 1385-1391.

[24] A.R.M. Hyyrylainen, J.M.H. Pakarinen, E. Forro, F. Fulop, P. Vainiotalo, Chiral differentiation of some cyclic beta-amino acids by kinetic and fixed ligand methods, J. Mass Spectrom., 45 (2010) 198-204.

[25] L.M. Wu, F.G. Vogt, D.Q. Liu, Flow-injection MS/MS for gas-phase chiral recognition and enantiomeric quantitation of a novel boron-containing antibiotic (GSK2251052A) by the mass spectrometric kinetic method, Anal. Chem., 85 (2013) 4869-4874.

[26] C.L. Gatlin, F. Turecek, T. Vaisar, Copper(II) amino acid complexes in the gas phase, J. Am. Chem. Soc., 117 (1995) 3637-3638.

[27] E.P.L. Hunter, S.G. Lias, Evaluated Gas Phase Basicities and Proton Affinities of Molecules: An Update, J. Phys. Chem. Ref. Data, 27 (1998) 413-656.

[28] M.M. Kish, G. Ohanessian, C. Wesdemiotis, The Na^+ affinities of α-amino acids: side-chain substituent effects, Int. J. Mass Spectrom., 227 (2003) 509-524.

[29] W.A. Tao, R.L. Clark, R.G. Cooks, Quotient ratio method for quantitative enantiomeric determination by mass spectrometry, Anal. Chem., 74 (2002) 3783-3789.

[30] W.A. Tao, F.C. Gozzo, R.G. Cooks, Mass spectrometric quantitation of chiral drugs by the kinetic method, Anal. Chem., 73 (2001) 1692-1698.

[31] D.X. Zhang, W.A. Tao, R.G. Cooks, Chiral resolution of D- and L-amino acids by tandem mass spectrometry of Ni(II)-bound trimeric complexes, Int. J. Mass Spectrom., 204 (2001) 159-169.

[32] V. Domalain, M. Hubert-Roux, C.M. Lange, J. Baudoux, J. Rouden, C. Afonso, Use of transition metals to improve the diastereomers differentiation by ion mobility and mass spectrometry, J. Mass Spectrom., 49 (2014) 423-427.

[33] T. Alizadeh, Enantioseparation of atenolol using chiral ligand-exchange chromatography on C_8 column, Sep. Purif. Technol., 118 (2013) 879-887.

[34] A. Rimola, L. Rodríguez-Santiago, M. Sodupe, Cation−π interactions and oxidative effects on Cu^{+} and Cu^{2+} binding to Phe, Tyr, Trp, and His Amino acids in the gas Phase. Insights from first-principles calculations, J. Phys. Chem. B, 110 (2006) 24189-24199.

[35] T. Wyttenbach, M. Witt, M.T. Bowers, On the stability of amino acid zwitterions in the gas phase: the influence of derivatization, proton affinity, and alkali ion addition, J. Am. Chem. Soc., 122 (2000) 3458-3464.

[36] W.A. Tao, D.X. Zhang, E.N. Nikolaev, R.G. Cooks, Copper(II)-assisted enantiomeric analysis of D,L-amino acids using the kinetic method: chiral recognition and quantification in the gas phase, J. Am. Chem. Soc., 122 (2000) 10598-10609.

[37] Z.P. Yao, T.S.M. Wan, K.P. Kwong, C.T. Che, Chiral analysis by electrospray ionization mass spectrometry/mass spectrometry. 2. Determination of enantiomeric excess of amino acids, Anal. Chem., 72 (2000) 5394-5401.

Table 1. Summary of the drift time, CCSs and resolutions of the significant chiral discrimination observed by IM-MS.

Y	X	Complex ion	m/z	Drift time (t) (ms)	Δt (ms)	CCS (Å^2)	ΔCCS (Å^2)	$R_{p\text{-}p}$[a]
His	Trp	$[(Cu^{2+})_2(^{L}X)(^{L}Y)_3\text{-}4H+Na]^+$	814	5.92±0.03	0.65±0.03	164.30	12.11	1.826±0.034
		$[(Cu^{2+})_2(^{D}X)(^{L}Y)_3\text{-}4H+Na]^+$		6.57±0.01		176.41		
	Gln	$[(Cu^{2+})_2(^{L}X)(^{L}Y)_3\text{-}4H+Na]^+$	756	5.46±0.01	0.48±0.01	155.56	9.15	1.411±0.043
		$[(Cu^{2+})_2(^{D}X)(^{L}Y)_3\text{-}4H+Na]^+$		5.94±0.01		164.71		
	Tyr	$[(Cu^{2+})_2(^{L}X)(^{L}Y)_3\text{-}4H+Na]^+$	791	5.78±0.02	0.54±0.02	161.74	10.16	1.398±0.029
		$[(Cu^{2+})_2(^{D}X)(^{L}Y)_3\text{-}4H+Na]^+$		6.32±0.01		171.90		
	Thr	$[(Cu^{2+})_2(^{L}X)(^{L}Y)_3\text{-}4H+Na]^+$	729	5.48±0.01	0.21±0.01	156.03	4.08	0.707±0.049
		$[(Cu^{2+})_2(^{D}X)(^{L}Y)_3\text{-}4H+Na]^+$		5.69±0.01		160.12		
Phe	His	$[(Cu^{2+})_2(^{L}X)(^{L}Y)_3\text{-}4H+Na]^+$	795	6.54±0.01	0.26±0.03	175.91	4.72	0.693±0.027
		$[(Cu^{2+})_2(^{D}X)(^{L}Y)_3\text{-}4H+Na]^+$		6.28±0.03		171.19		
Trp	Gln	$[(Cu^{2+})_2(^{L}X)(^{L}Y)_3\text{-}4H+Na]^+$	903	6.81±0.01	0.59±0.01	180.83	10.49	1.519±0.030
		$[(Cu^{2+})_2(^{D}X)(^{L}Y)_3\text{-}4H+Na]^+$		7.40±0.01		191.31		
	Tyr	$[(Cu^{2+})_2(^{L}X)(^{L}Y)_3\text{-}4H+Na]^+$	938	6.99±0.02	0.56±0.02	183.97	9.85	1.234±0.015
		$[(Cu^{2+})_2(^{D}X)(^{L}Y)_3\text{-}4H+Na]^+$		7.55±0.01		193.82		
	Glu	$[(Cu^{2+})_2(^{L}X)(^{L}Y)_3\text{-}4H+Na]^+$	904	6.86±0.01	0.48±0.01	181.58	8.49	1.190±0.031
		$[(Cu^{2+})_2(^{D}X)(^{L}Y)_3\text{-}4H+Na]^+$		7.33±0.01		190.07		
	Met	$[(Cu^{2+})_2(^{L}X)(^{L}Y)_3\text{-}4H+Na]^+$	906	7.16±0.01	0.37±0.01	187.02	6.45	0.887±0.013
		$[(Cu^{2+})_2(^{D}X)(^{L}Y)_3\text{-}4H+Na]^+$		7.53±0.01		193.47		
	Phe	$[(Cu^{2+})_2(^{L}X)(^{L}Y)_3\text{-}4H+Na]^+$	922	7.30±0.01	0.30±0.01	189.52	5.19	0.692±0.016
		$[(Cu^{2+})_2(^{D}X)(^{L}Y)_3\text{-}4H+Na]^+$		7.60±0.01		194.71		
Tyr	Glu	$[(Cu^{2+})_2(^{L}X)(^{L}Y)_2\text{-}4H+Na]^+$ [b]	654	5.19±0.01	0.29±0.01	150.32	5.75	1.037±0.012
		$[(Cu^{2+})_2(^{D}X)(^{L}Y)_2\text{-}4H+Na]^+$ [b]		4.90±0.01		144.57		
	Arg	$[(Cu^{2+})_2(^{L}X)(^{L}Y)_3\text{-}3H]^+$	840	6.99±0.01	0.37±0.01	184.07	6.68	1.015±0.006
		$[(Cu^{2+})_2(^{D}X)(^{L}Y)_3\text{-}3H]^+$		6.62±0.01		177.39		
	His	$[(Cu^{2+})_2(^{L}X)(^{L}Y)_3\text{-}4H+Na]^+$	843	7.05±0.01	0.25±0.01	185.05	4.46	0.687±0.018
		$[(Cu^{2+})_2(^{D}X)(^{L}Y)_3\text{-}4H+Na]^+$		6.80±0.01		180.59		

[a] The $R_{p\text{-}p}$ value was calculated using the racemic anlayte. [b] Obvious chiral discrimination was observed for the binuclear copper bound trimeric ion instead.

Table 2. Summary of chiral discrmination observed by MS/MS study of $[(Cu^{2+})_2(^{L/D}X)(^{L}Trp)_3\text{-}4H+Na]^+$ ions.

X		Collision energy (eV)	Intensity ratio of $[(Cu^{2+})_2(X)(Trp)_2\text{-}4H+Na]^+$ to $[(Cu^{2+})_2(X)(Trp)_3\text{-}4H+Na]^+$		
			r_L	r_D	Enantioselectivity (r_D/r_L)
aromatic	Phe	20	0.153±0.003	0.252±0.007	1.645±0.059
	Tyr	15	0.118±0.004	0.200±0.011	1.700±0.108
cyclic	Pro	20	0.140±0.011	0.516±0.010	3.684±0.302
basic	Arg	17	0.941±0.031	2.010±0.122	2.136±0.147
	His	23	1.318±0.036	2.087±0.063	1.584±0.065
	Lys	20	0.215±0.014	0.564±0.038	2.618±0.242
acid and their amide	Asn	22	0.958±0.075	1.416±0.105	1.477±0.159
	Asp	12	0.927±0.028	2.066±0.053	2.228±0.089
	Gln	20	0.147±0.008	0.289±0.007	1.973±0.122
	Glu	11	0.976±0.023	1.247±0.050	1.277±0.060
aliphatic	Ala[a]	16	1.260±0.026	1.302±0.020	1.034±0.027
	Ile[b]	20	0.517±0.043	0.656±0.034	1.269±0.125
	Leu[b]	20	0.669±0.028	0.571±0.043	1.172±0.102
	Val[b]	19	0.334±0.007	0.394±0.017	1.179±0.056
hydroxyl or sulfur containing	Met	20	0.170±0.010	0.626±0.020	3.683±0.239
	Ser	16	1.152±0.039	4.432±0.246	3.849±0.251
	Thr	17	2.205±0.071	4.583±0.263	2.078±0.136

[a] The intensity ratio of $[(Cu^{+})_2(Trp)_2\text{-}2H+Na]^+$to $[(Cu^{2+})_2(X)(Trp)_3\text{-}4H+Na]^+$ was used for chiral recognition instead since the product ion $[(Cu^{2+})_2(X)(Trp)_2\text{-}4H+Na]^+$ was of too low intensity to be effectively detected (see Fig. S4).

[b] The intensity ratio of $[(Cu^{+})_2(X)(Trp)\text{-}2H+Na]^+$ to $[(Cu^{2+})_2(X)(Trp)_3\text{-}4H+Na]^+$ was used for chiral recognition instead since the product ion $[(Cu^{2+})_2(X)(Trp)_2\text{-}4H+Na]^+$ was of too low intensity to be effectively detected (see Fig. S4).

Table 3. Enantiomeric excess measurements of Trp samples.[a]

Actual ee of sample	Measured ee						Mean±SD	RSD (%)	Absolute error
	1	2	3	4	5	6			
50	46.75	47.40	50.36	48.84	48.80	52.54	49.12±2.10	1.76	0.88
10	11.42	6.85	9.75	9.78	7.38	10.94	9.35±1.86	3.67	0.65
0	-2.76	-2.07	-3.16	-1.85	-2.68	0.33	-2.07±3.16	—	2.07
-10	-10.29	-9.38	-9.57	-10.46	-9.52	-8.57	-9.63±0.68	6.45	0.37
-50	-47.79	-50.75	-52.08	-47.74	-51.78	-52.65	-50.47±2.18	0.93	0.47

[a] The solution for IM-MS analysis contained 20 μM Trp, 20 μM L-His and 20 μM $CuCl_2$.

FIGURE CAPTIONS

Fig. 1. Mass spectrum obtained for a mixture containing 20 μM His, 20 μM Trp and 20 μM $CuCl_2$.

Fig. 2. Ion mobility spectra for $[(Cu^{2+})_2{}^{L/D}X(^{L}Trp)_3\text{-}4H+Na]^+$ (X = Tyr (a), Phe (b), Gln (c), Glu (d), Met (e)) and $[(Cu^{2+})_2{}^{L/D}X(^{L}His)_3\text{-}4H+Na]^+$ (X = Trp (f); Tyr (g); Gln (h); Thr (i)). The concentration of each enantiomer of analyte was 10 μM. Inset in (a) is the monoisotopic peak of the diastereomeric ion extracted for the IM-MS analysis. Similar monoisotopic peaks were extracted for IM-MS analysis of other diastereomeric ions.

Fig. 3. Ion mobility spectra for $[(Cu^{2+})_2{}^{L/D}Arg(^{L}Tyr)_3\text{-}3H]^+$ (a), $[(Cu^{2+})_2{}^{L/D}Glu(^{L}Tyr)_2\text{-}4H+Na]^+$ (b), $[(Cu^{2+})_2{}^{L/D}His(^{L}Tyr)_3\text{-}4H+Na]^+$ (c) and $[(Cu^{2+})_2{}^{L/D}His(^{L}Phe)_3\text{-}4H+Na]^+$ (d). The concentration of each enantiomer of the analyte was 10 μM.

Fig. 4. Drift time plot obtained for a pair of diastereomeirc ions (a: $[(Cu^{2+})_2{}^{L/D}Trp(^{L}His)_3\text{-}4H+Na]^+$, c: $[(Cu^{2+})_2{}^{L/D}Arg(^{L}Tyr)_3\text{-}3H]^+$, e: $[(Cu^{2+})_2{}^{L/D}Glu(^{L}Tyr)_2\text{-}4H+Na]^+$), and plot of *r* against 1/(100-ee) (b: $[(Cu^{2+})_2{}^{L/D}Trp(^{L}His)_3\text{-}4H+Na]^+$, d: $[(Cu^{2+})_2{}^{L/D}Arg(^{L}Tyr)_3\text{-}3H]^+$, f: $[(Cu^{2+})_2{}^{L/D}Glu(^{L}Tyr)_2\text{-}4H+Na]^+$). The peak areas were obtained by peak fitting using OriginPro software (version 8.0).

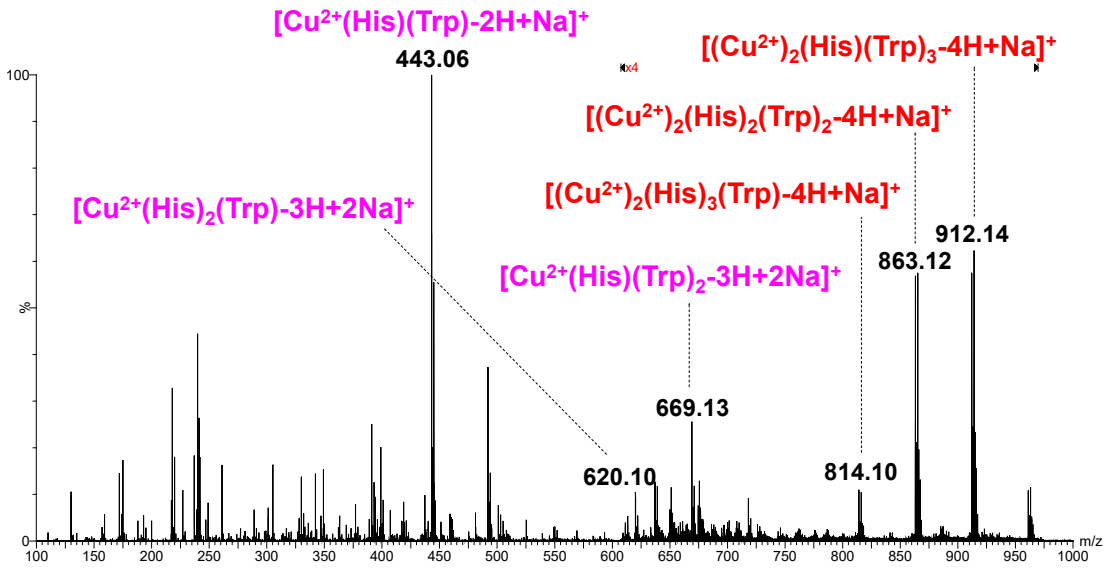
[Cu2+(His)(Trp)-2H+Na]+
443.06
[(Cu2+)2(His)(Trp)3-4H+Na]+
x4
[(Cu2+)2(His)2(Trp)2-4H+Na]+
[(Cu2+)2(His)3(Trp)-4H+Na]+
[Cu2+(His)2(Trp)-3H+2Na]+
912.14
863.12
[Cu2+(His)(Trp)2-3H+2Na]+
669.13
620.10
814.10
100
%
0
100 150 200 250 300 350 400 450 500 550 600 650 700 750 800 850 900 950 1000
m/z

Fig. 1.

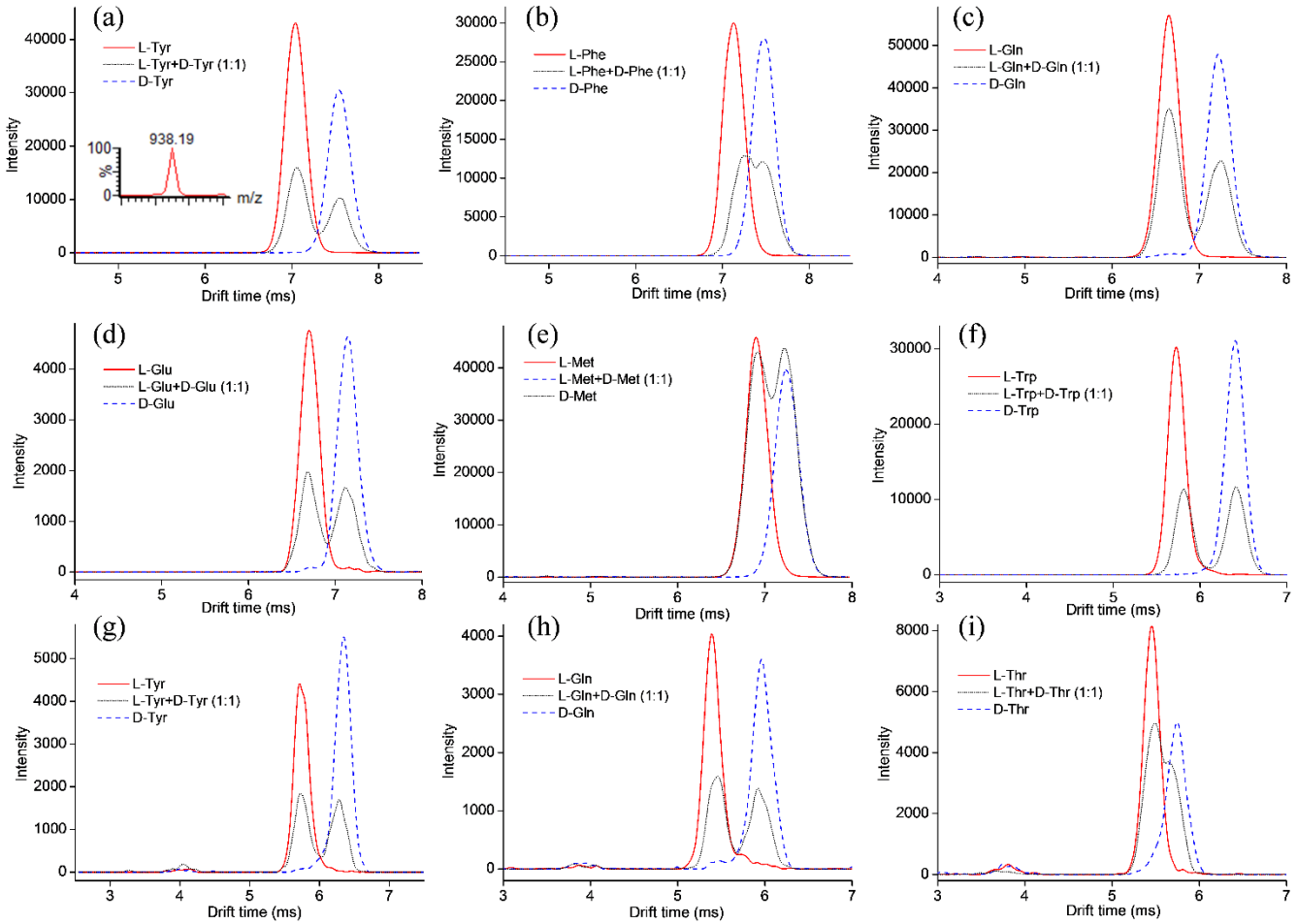
(a)
L-Tyr
L-Tyr+D-Tyr (1:1)
D-Tyr
938.19
100
%
0
m/z
Intensity
Drift time (ms)
(b)
L-Phe
L-Phe+D-Phe (1:1)
D-Phe
(c)
L-Gln
L-Gln+D-Gln (1:1)
D-Gln
(d)
L-Glu
L-Glu+D-Glu (1:1)
D-Glu
(e)
L-Met
L-Met+D-Met (1:1)
D-Met
(f)
L-Trp
L-Trp+D-Trp (1:1)
D-Trp
(g)
L-Tyr
L-Tyr+D-Tyr (1:1)
D-Tyr
(h)
L-Gln
L-Gln+D-Gln (1:1)
D-Gln
(i)
L-Thr
L-Thr+D-Thr (1:1)
D-Thr

Fig.2.

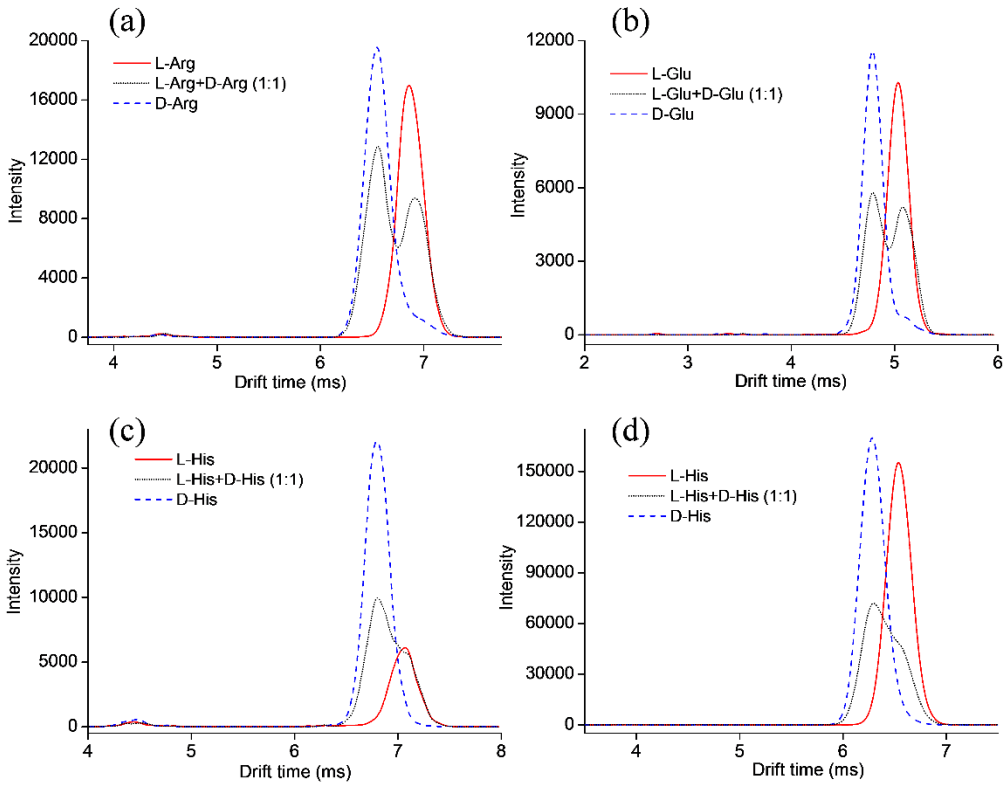
(a)
L-Arg
L-Arg+D-Arg (1:1)
D-Arg
Intensity
Drift time (ms)
(b)
L-Glu
L-Glu+D-Glu (1:1)
D-Glu
Intensity
Drift time (ms)
(c)
L-His
L-His+D-His (1:1)
D-His
Intensity
Drift time (ms)
(d)
L-His
L-His+D-His (1:1)
D-His
Intensity
Drift time (ms)

Fig. 3.

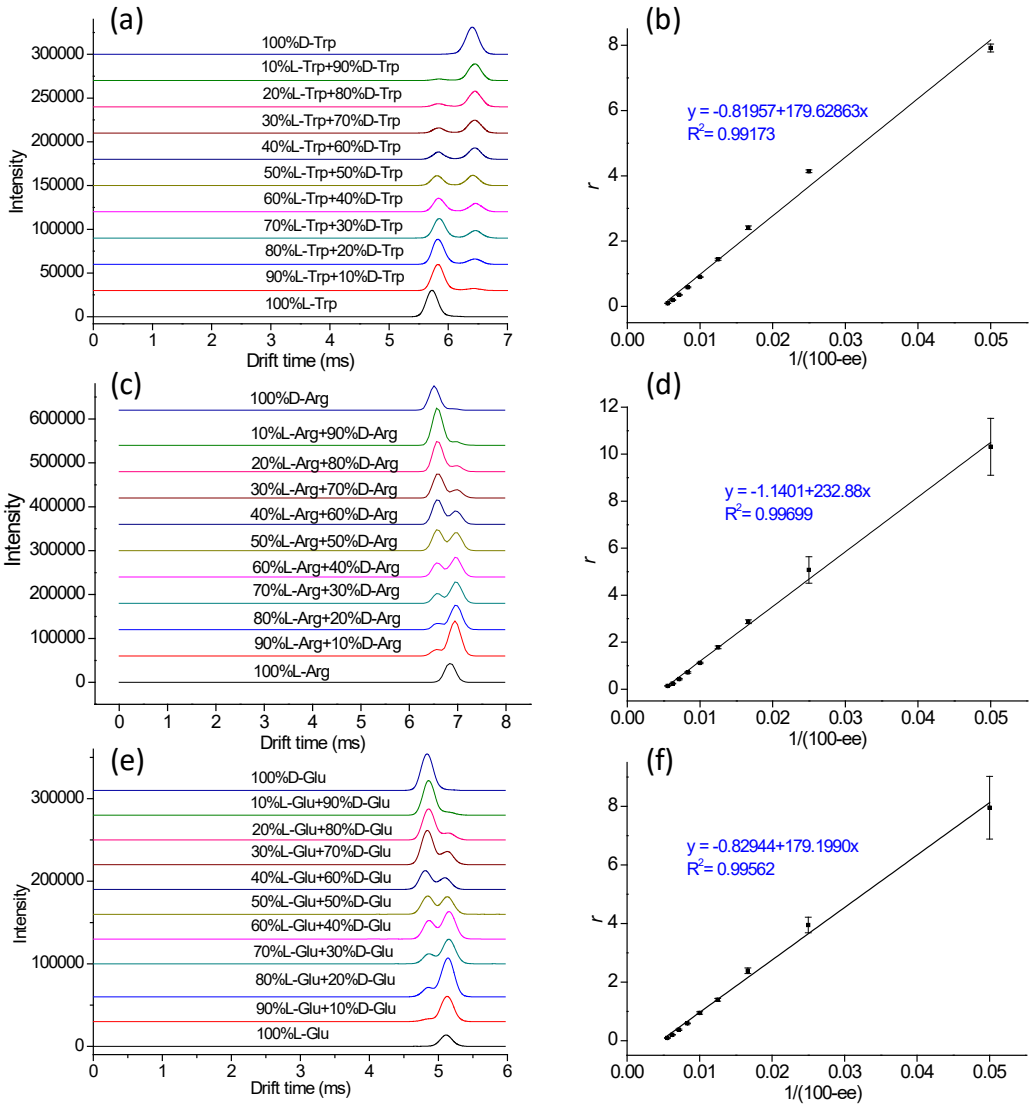
(a)
100%D-Trp
10%L-Trp+90%D-Trp
20%L-Trp+80%D-Trp
30%L-Trp+70%D-Trp
40%L-Trp+60%D-Trp
50%L-Trp+50%D-Trp
60%L-Trp+40%D-Trp
70%L-Trp+30%D-Trp
80%L-Trp+20%D-Trp
90%L-Trp+10%D-Trp
100%L-Trp
Intensity
Drift time (ms)
(b)
y = -0.81957+179.62863x
R2= 0.99173
r
1/(100-ee)
(c)
100%D-Arg
10%L-Arg+90%D-Arg
20%L-Arg+80%D-Arg
30%L-Arg+70%D-Arg
40%L-Arg+60%D-Arg
50%L-Arg+50%D-Arg
60%L-Arg+40%D-Arg
70%L-Arg+30%D-Arg
80%L-Arg+20%D-Arg
90%L-Arg+10%D-Arg
100%L-Arg
Intensity
Drift time (ms)
(d)
y = -1.1401+232.88x
R2= 0.99699
r
1/(100-ee)
(e)
100%D-Glu
10%L-Glu+90%D-Glu
20%L-Glu+80%D-Glu
30%L-Glu+70%D-Glu
40%L-Glu+60%D-Glu
50%L-Glu+50%D-Glu
60%L-Glu+40%D-Glu
70%L-Glu+30%D-Glu
80%L-Glu+20%D-Glu
90%L-Glu+10%D-Glu
100%L-Glu
Intensity
Drift time (ms)
(f)
y = -0.82944+179.1990x
R2= 0.99562
r
1/(100-ee)

Fig. 4.